Electronic Supporting Information

Anionic sulfonated and carboxylated PPI dendrimers with EDA core: synthesis and characterization as selective metal complexing agents

Sandra García-Gallego,[a] Michela Cangiotti,[b] Luigi Fiorani,[b] Alberto Fattori,[b] Mª Ángeles Muñoz-Fernández,*[c] Rafael Gomez,*[a] Mª Francesca Ottaviani*[b] and F. Javier de la Mata.*[a]

[a] S. García-Gallego, Dr. R. Gómez, Dr. F. J. De la Mata
Departamento de Química Inorgánica, Universidad de Alcalá, Campus Universitario, E-28871 Alcalá de Henares (Spain). Networking Research Center on Bioengineering, Biomaterials and Nanomedicine (CIBER-BBN), Spain.
E-mail: javier.delamata@uah.es

[b] Dr. M. Cangiotti, L. Fiorani, A. Fattori, Dr. M. F. Ottaviani
Department of Earth, Life and Environment Sciences, 61029 Urbino (Italy).
E-mail: maria.ottaviani@uniurb.it

[c] Dr. M. A. Muñoz-Fernández
Laboratorio de Inmunobiología Molecular, Hospital General Universitario Gregorio Marañón, Madrid (Spain). Networking Research Center on Bioengineering, Biomaterials and Nanomedicine (CIBER-BBN), Spain.
E-mail: mmunoz.hgugm@salud.madrid.org

Table of Contents Page Number

- **EPR spectra**

- **NMR spectra**

- ## UV-Vis spectra

- ## Potentiometric titration study

- **EPR spectra**

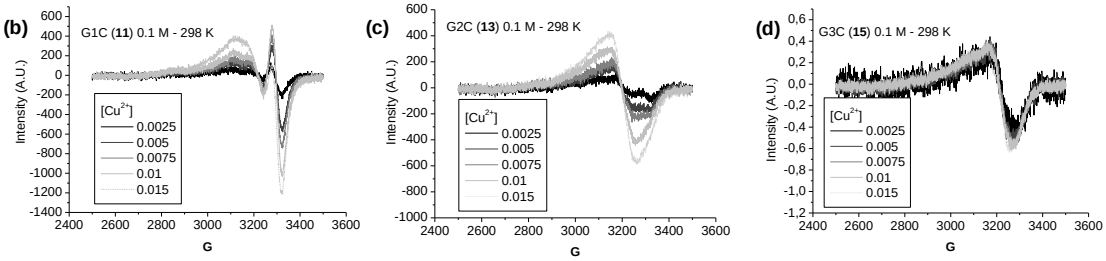

Figure S1. Experimental EPR spectra of carboxylate dendrimers **11**, **13** and **15** at 298 K, with increasing copper concentration (0.0025-0.015 M).

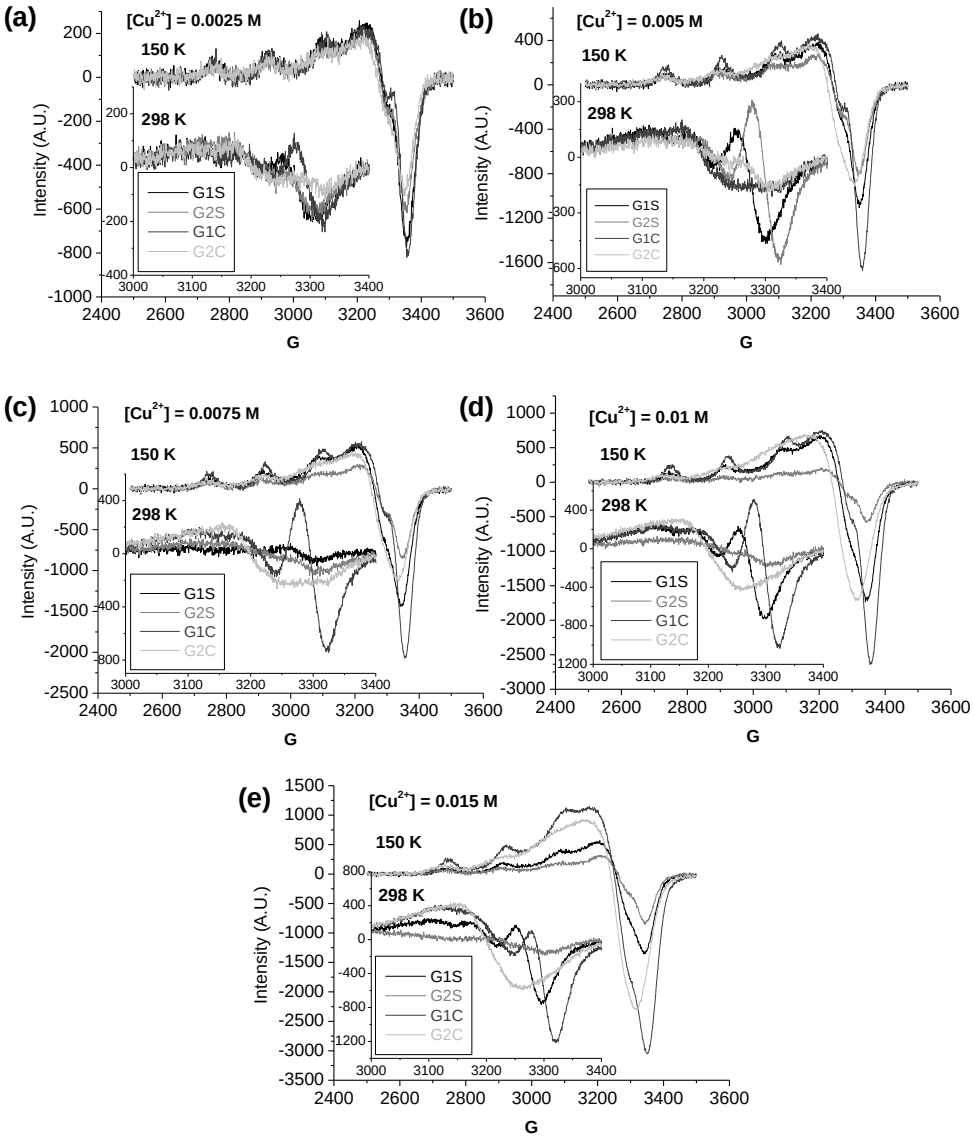

Figure S2. Comparative experimental EPR spectra at room and low temperature of carboxylate **11**, **13** and **15** and sulfonate **7**, **8** and **9** dendrimers, with increasing copper concentration (0.0025-0.015 M).

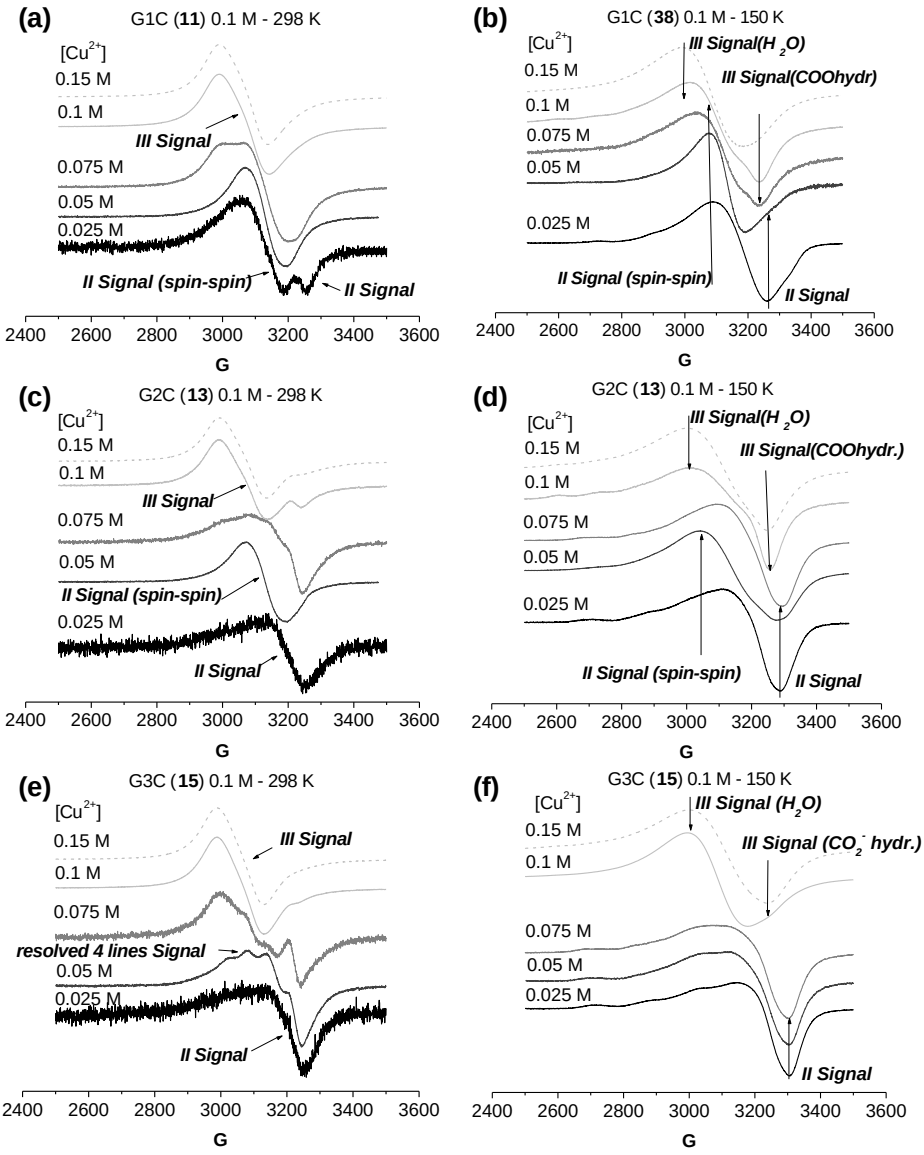

Figure S3. Experimental EPR spectra of carboxylate dendrimers **11**, **13** and **15**, at 298 K (left) and 150 K (right), with increasing copper concentration (0.025-0.15M).

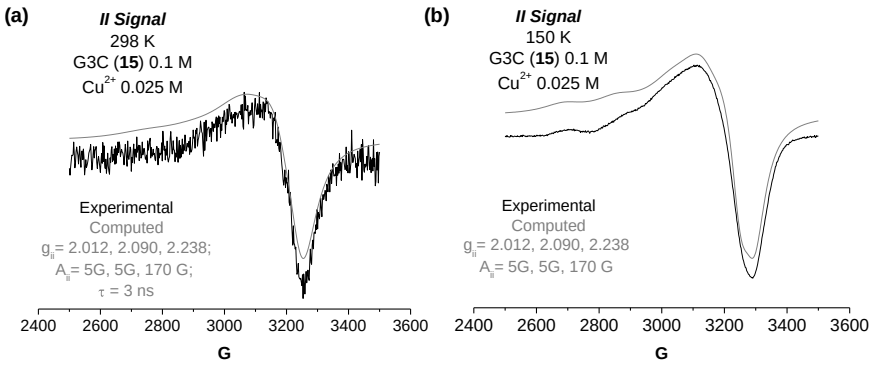

Figure S4. Experimental (black) and computed (grey) EPR spectra of carboxylate dendrimer G3C (**15**), at 298 K (left) and 150 K (right).

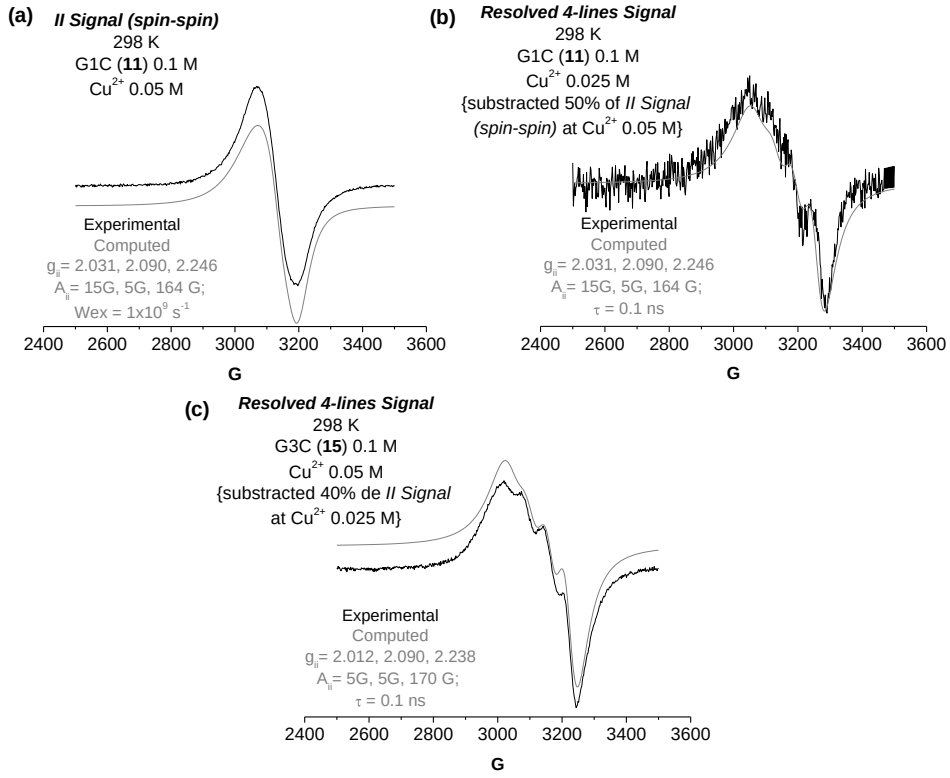

Figure S5. Experimental (black) and computed (grey) EPR spectra of carboxylate dendrimers G1C (**11**) and G3C (**15**), at 298 K.

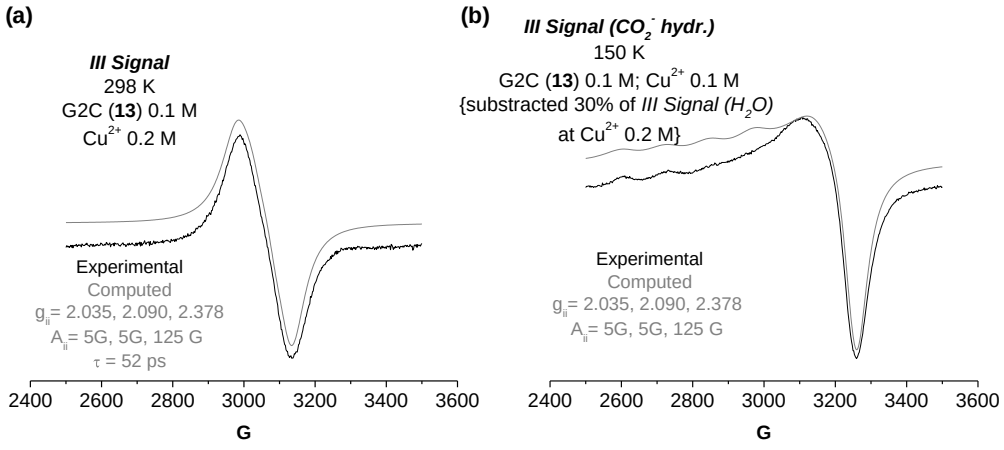

Figure S6. *II Signal* in experimental (black) and computed (grey) EPR spectra of carboxylate dendrimer G2C (**13**) at 298 and 150 K.

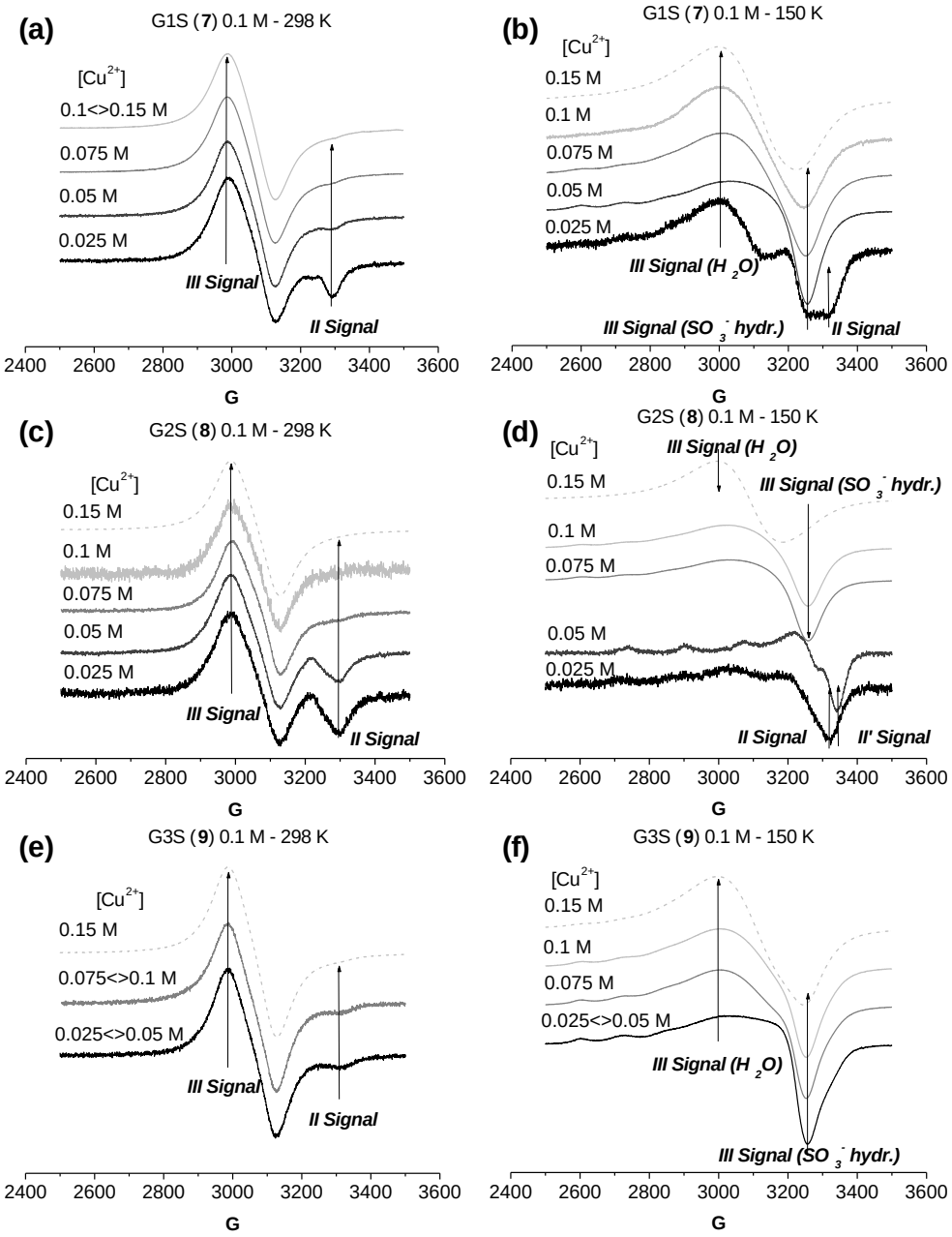

Figure S7. Experimental EPR spectra of sulfonate dendrimers **7**, **8** and **9**, at 298 K (left) and 150 K (right), at increasing copper concentration (0.025-0.15M).

- **NMR spectra**

A) EDA-*dendr*-$(SO_3Na)_8$ (7)

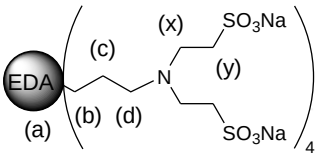

(**7**)

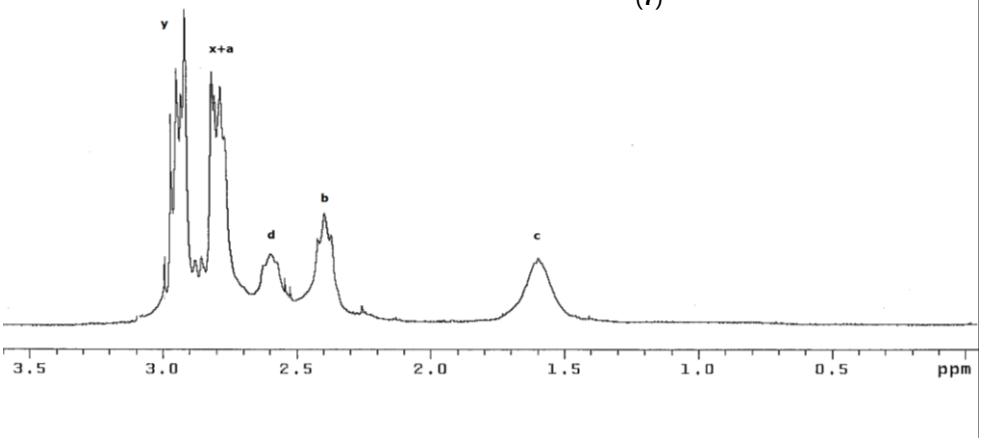

Figure S8. ^{1}H NMR spectrum of EDA-dendr-$(SO3Na)_8$ (**7**) in D_2O.

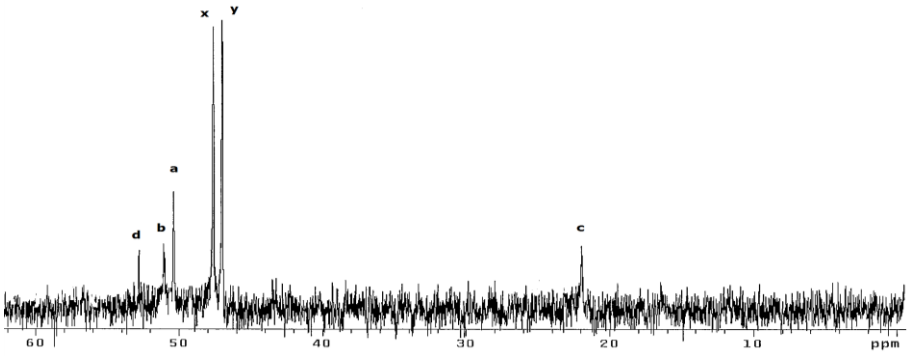

Figure S9. ^{13}C NMR spectrum of EDA-dendr-$(SO3Na)_8$ (**7**) in D_2O.

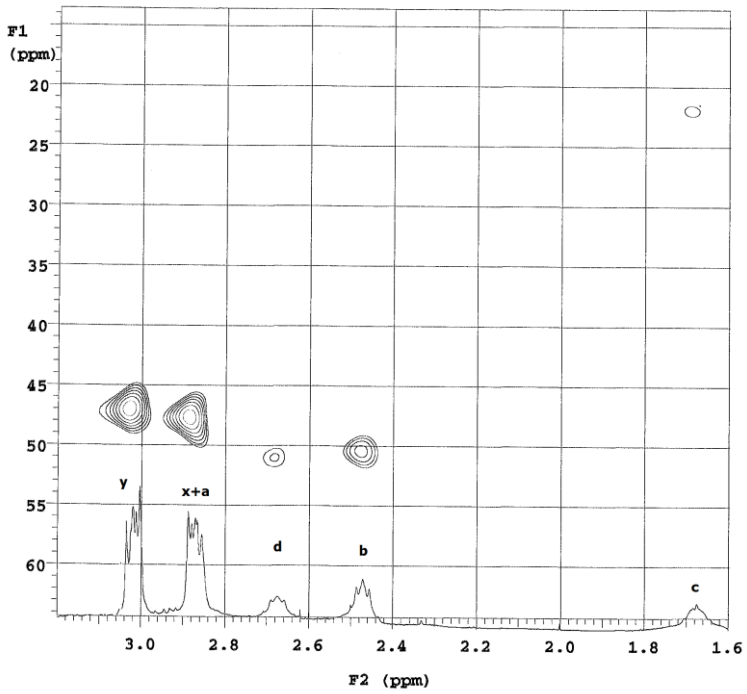

Figure S10. ^{1}H-^{13}C-{HMQC} NMR spectrum of EDA-dendr-$(SO3Na)_8$ (**7**) in D_2O.

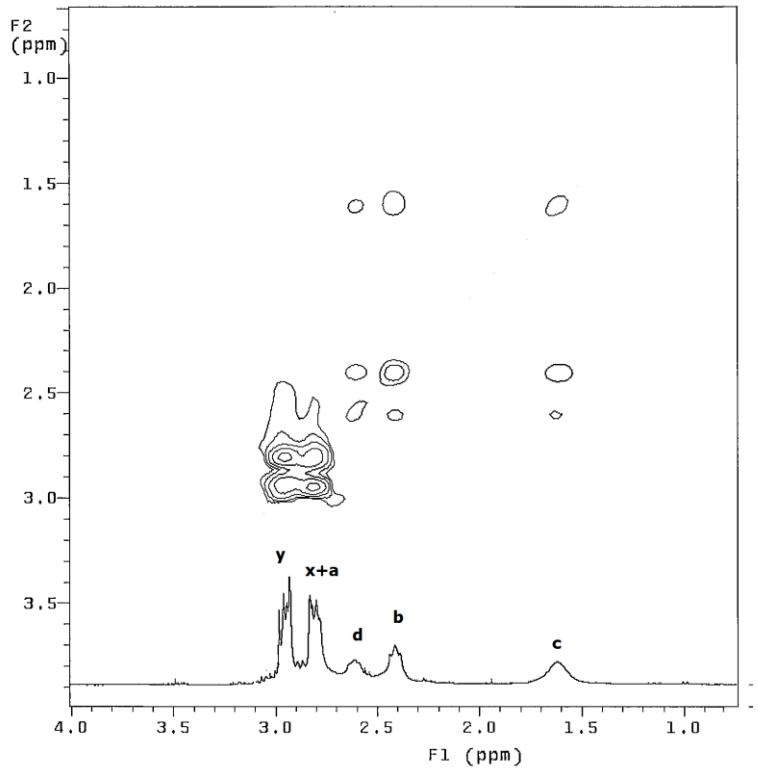

Figure S11. NOESY ^{1}H-NMR spectrum of EDA-dendr-$(SO3Na)_8$ (**7**) in D_2O.

B) EDA-*dendr*-$(SO_3Na)_{16}$ (8)

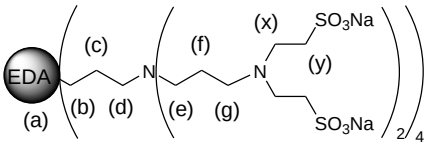

(**8**)

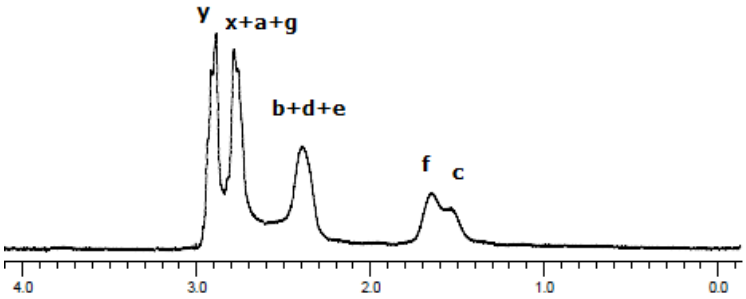

Figure S12. ^{1}H NMR spectrum of EDA-*dendr*-$(SO_3Na)_{16}$ (**8**) in D_2O.

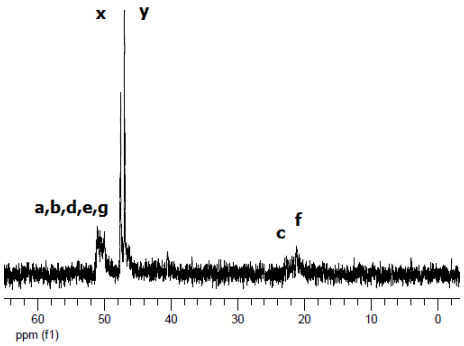

Figure S13. ^{13}C NMR spectrum of EDA-*dendr*-$(SO_3Na)_{16}$ (**8**) in D_2O.

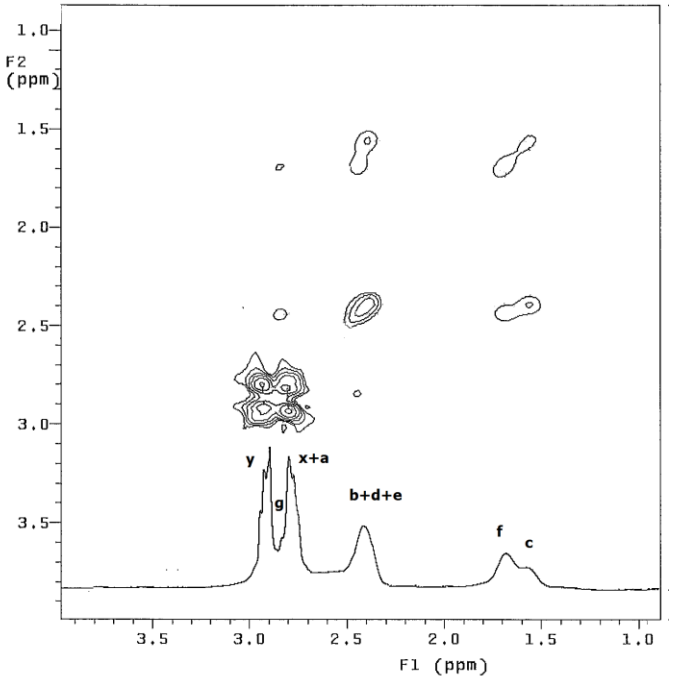

Figure S14. TOCSY NMR spectrum of EDA-*dendr*-$(SO_3Na)_{16}$ (**8**) in D_2O.

C) EDA-*dendr*-$(SO_3Na)_{32}$ (9)

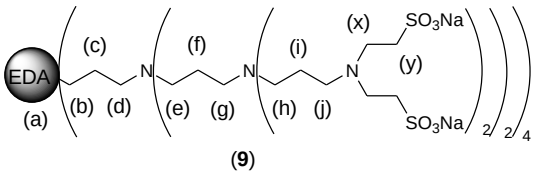

(**9**)

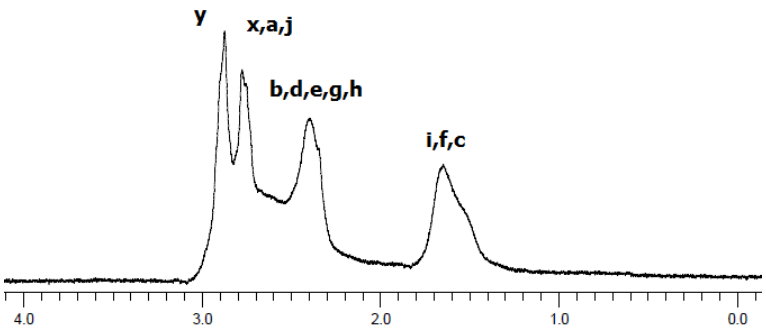

Figure S15. ^{1}H NMR spectrum of EDA-*dendr*-$(SO_3Na)_{32}$ (**9**) in D_2O.

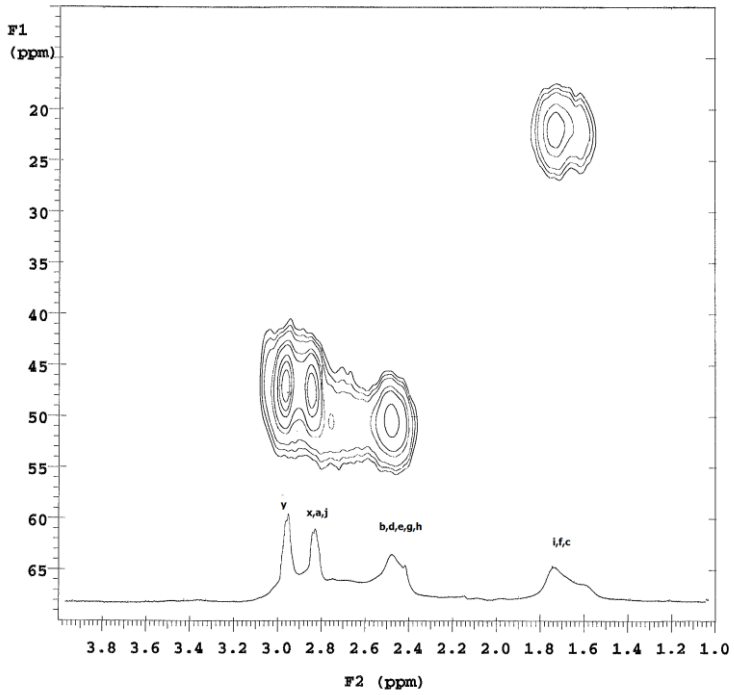

Figure S16. ^{1}H-^{13}C-{HMQC} NMR spectrum of EDA-*dendr*-$(SO_3Na)_{32}$ (**9**) in D_2O..

D) EDA-*dendr*-$(CO_2Me)_8$ (10)

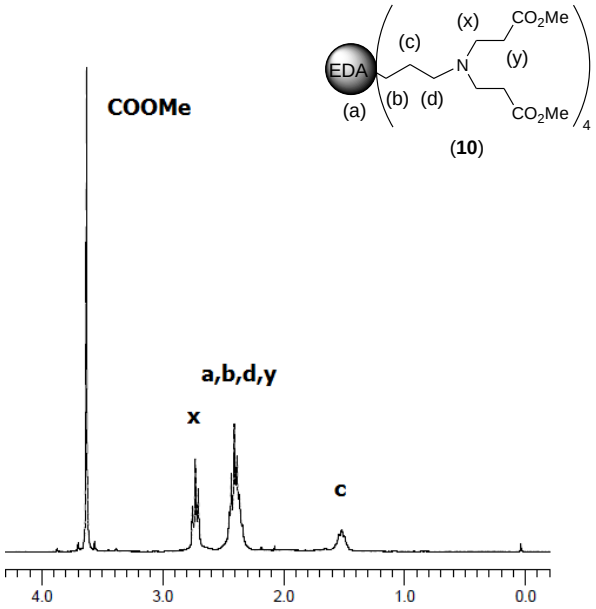

Figure S17. ^{1}H NMR spectrum of EDA-*dendr*-$(CO_2Me)_8$ (**10**) in $CDCl_3$.

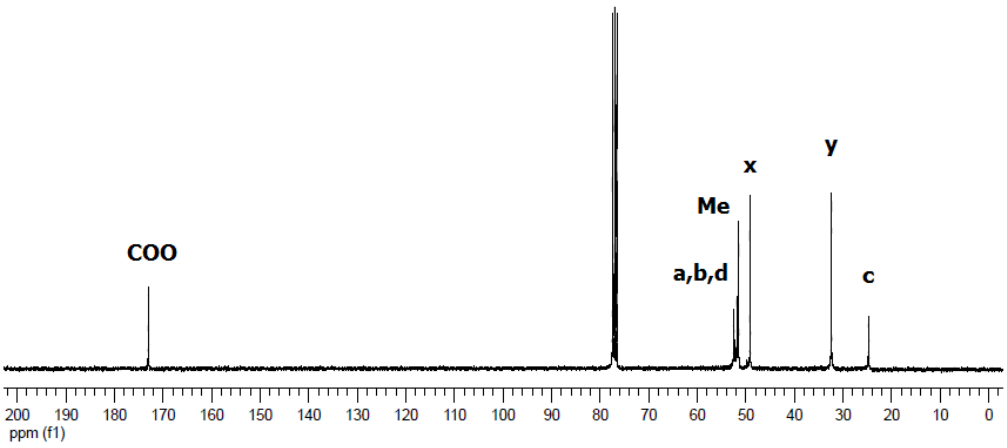

Figure S18. ^{13}C NMR spectrum of EDA-*dendr*-$(CO_2Me)_8$ (**10**) in $CDCl_3$.

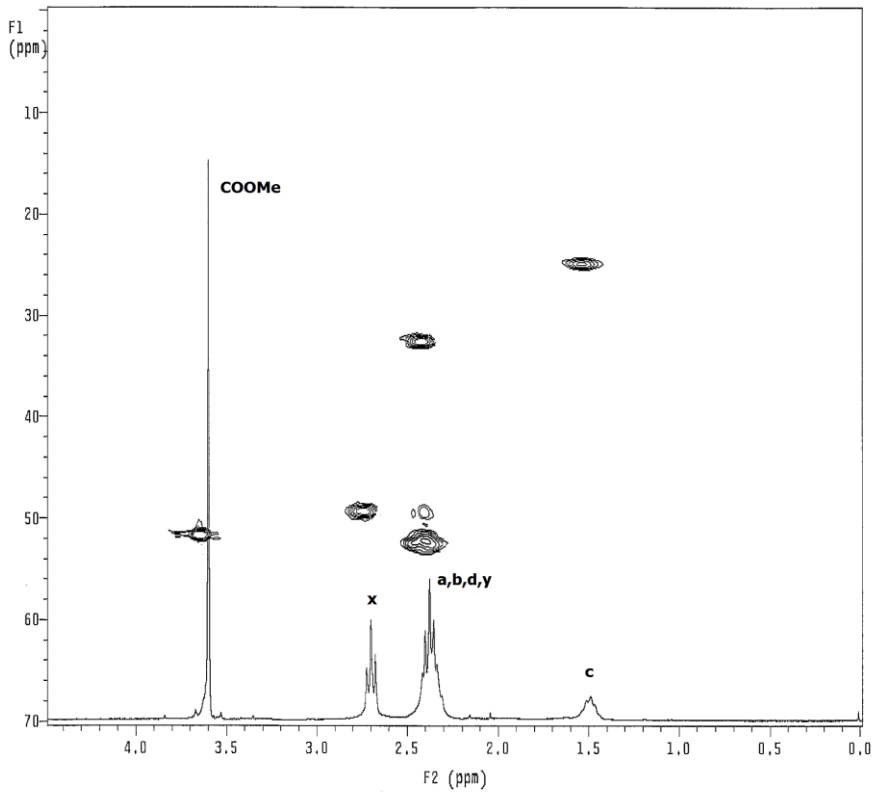

Figure S19. ^{1}H-^{13}C-{HMQC} NMR spectrum of EDA-*dendr*-$(CO_2Me)_8$ (**10**) in $CDCl_3$

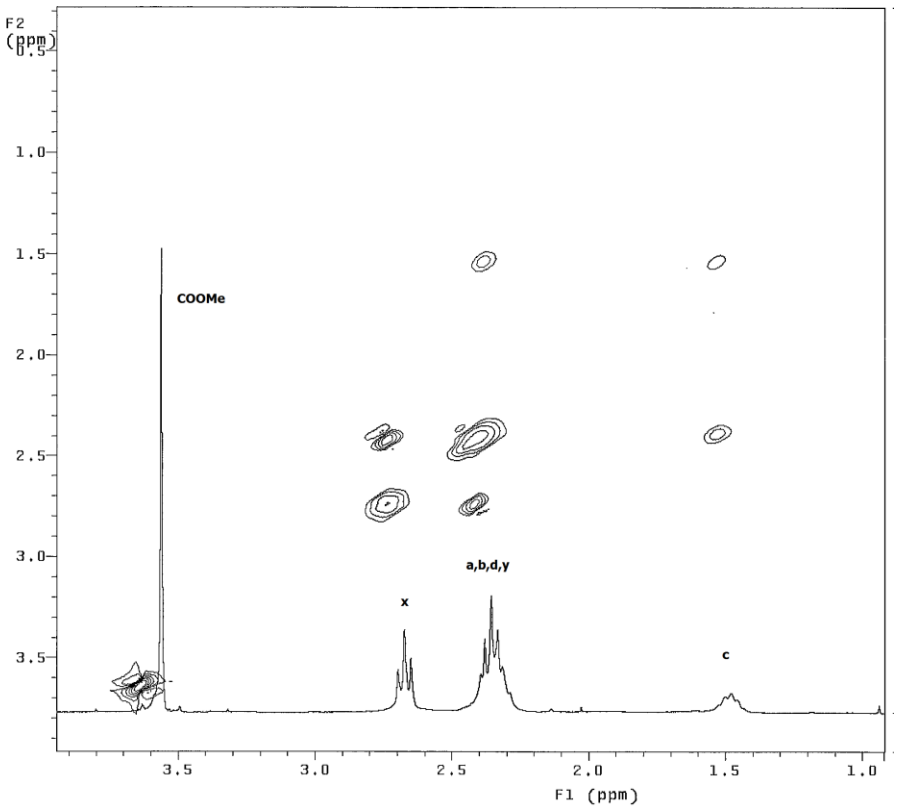

Figure S20. NOESY ^{1}H-NMR spectrum of EDA-*dendr*-$(CO_2Me)_8$ (**10**) in $CDCl_3$.

E) EDA-*dendr*-$(CO_2Na)_8$ (11)

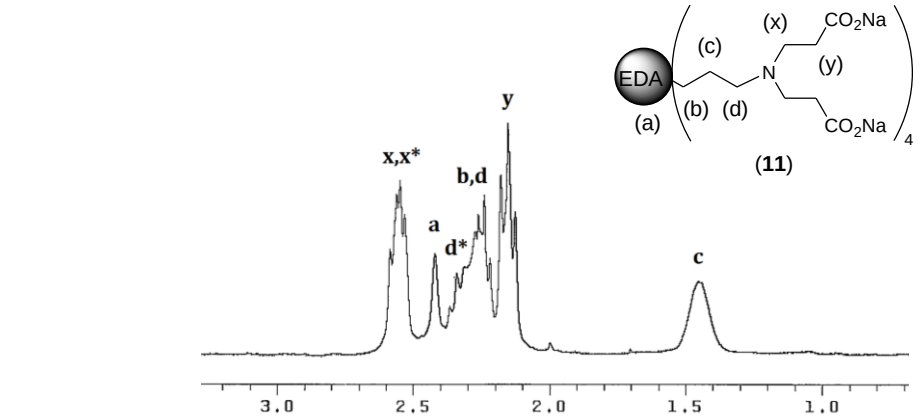

Figure S21. ^{1}H NMR spectrum of EDA-*dendr*-$(CO_2Na)_8$ (**11**) in D_2O.

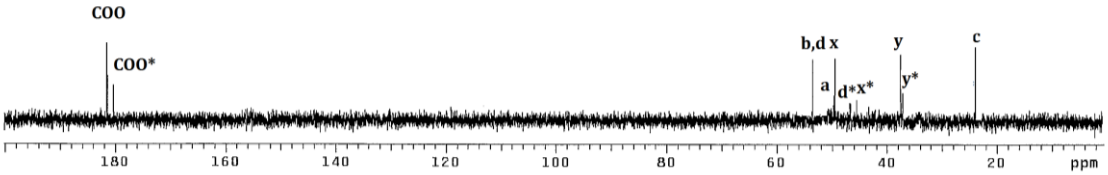

Figure S22. ^{13}C NMR spectrum of EDA-*dendr*-$(CO_2Na)_8$ (**11**) in D_2O.

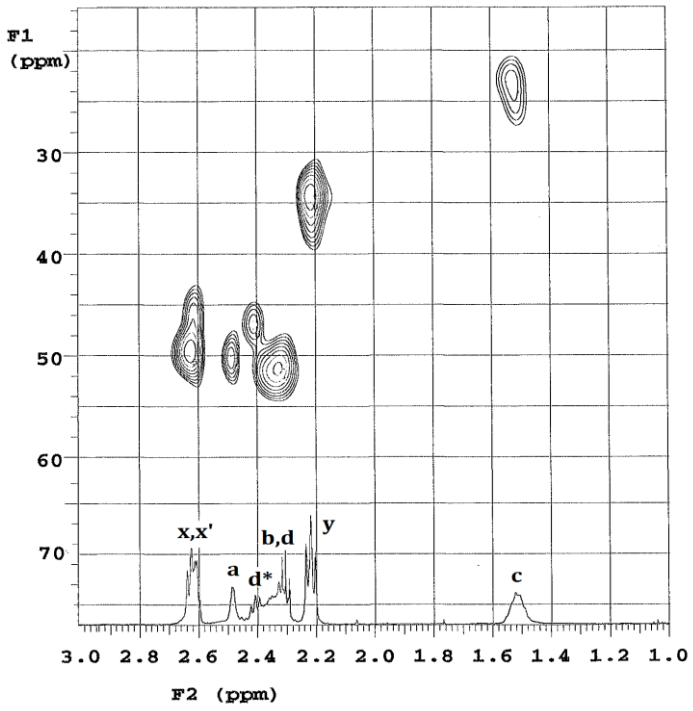

Figure S23. ^{1}H-^{13}C-{HSQC} NMR spectrum of EDA-*dendr*-$(CO_2Na)_8$ (**11**) in D_2O

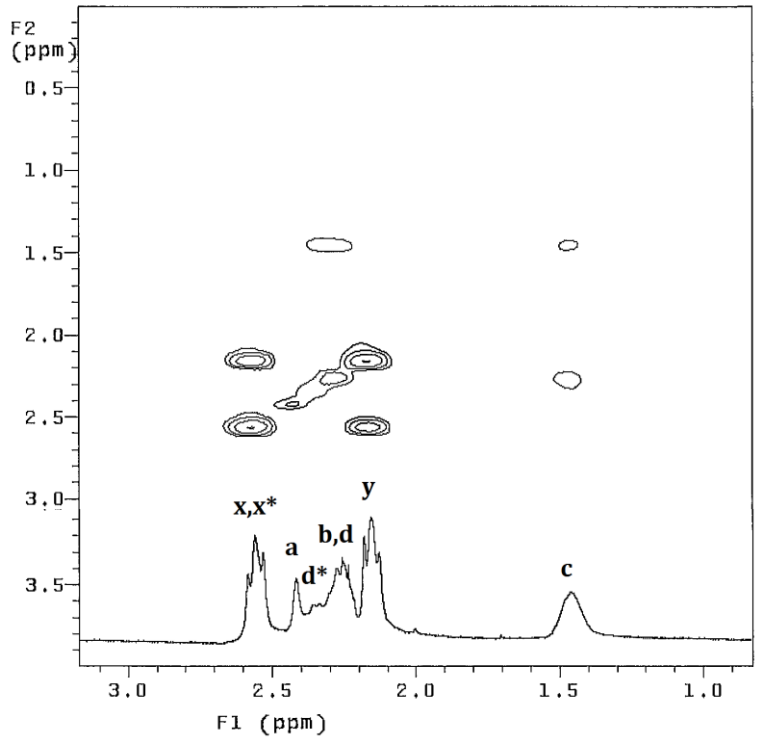

Figure S24. TOCSY ^{1}H-NMR spectrum of EDA-*dendr*-$(CO_2Na)_8$ (**11**) in D_2O.

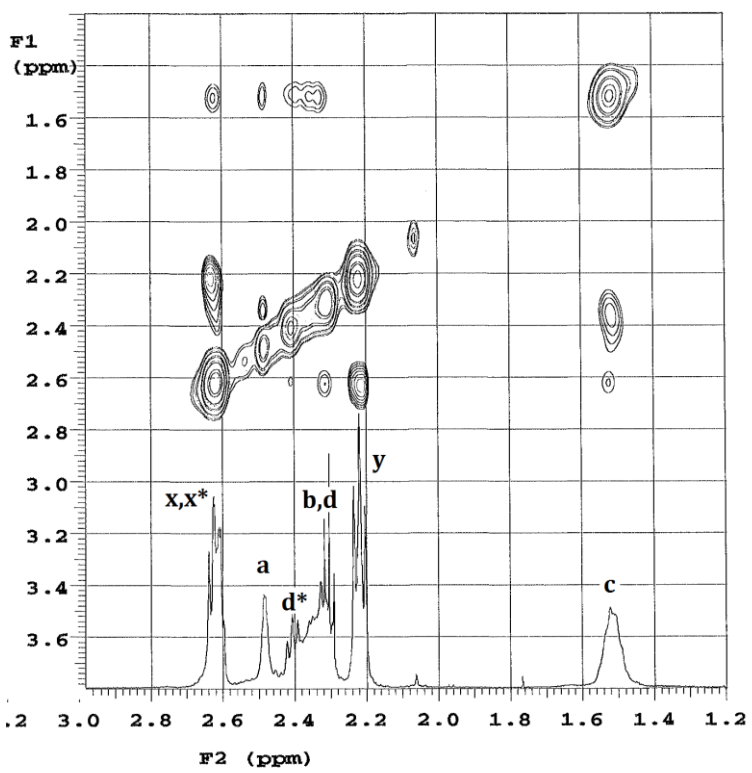

Figure S25. ROESY NMR spectrum of EDA-*dendr*-$(CO_2Na)_8$ (**11**) in D_2O.

F) EDA-*dendr*-$(CO_2Me)_{16}$ (12)

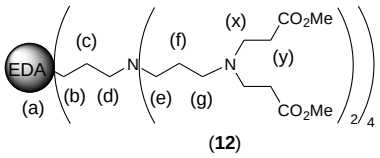

(**12**)

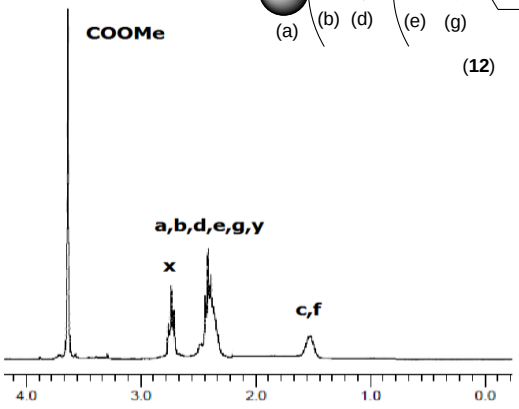

Figure S26. ^{1}H NMR spectrum of EDA-*dendr*-$(CO_2Me)_{16}$ (**12**) in $CDCl_3$.

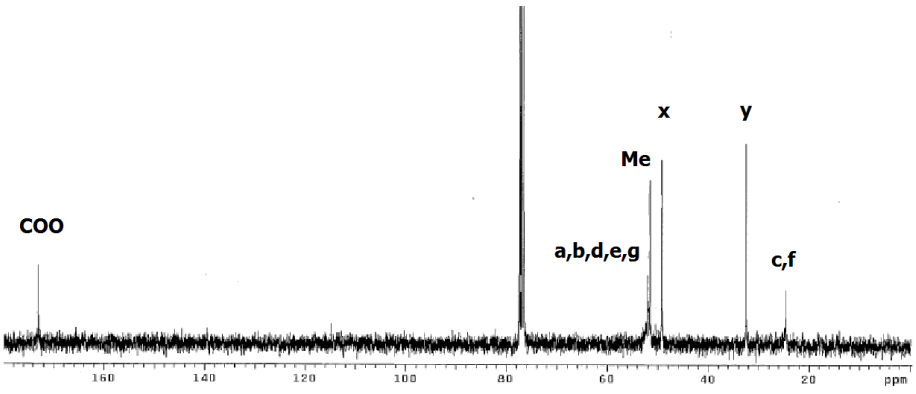

Figure S27. ^{13}C NMR spectrum of EDA-*dendr*-$(CO_2Me)_{16}$ (**12**) in $CDCl_3$.

G) EDA-*dendr*-$(CO_2Na)_{16}$ (13)

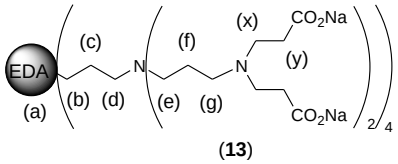

(**13**)

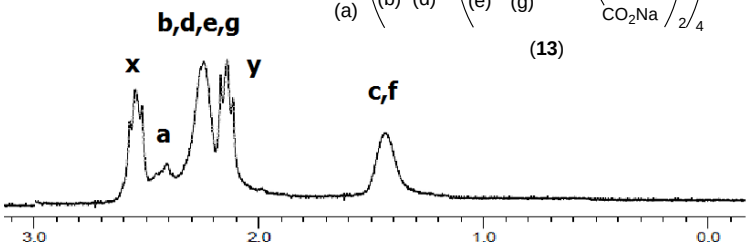

Figure S28. ^{1}H NMR spectrum of EDA-*dendr*-$(CO_2Na)_{16}$ (**13**) in D_2O.

H) EDA-*dendr*-$(CO_2Me)_{32}$ (14)

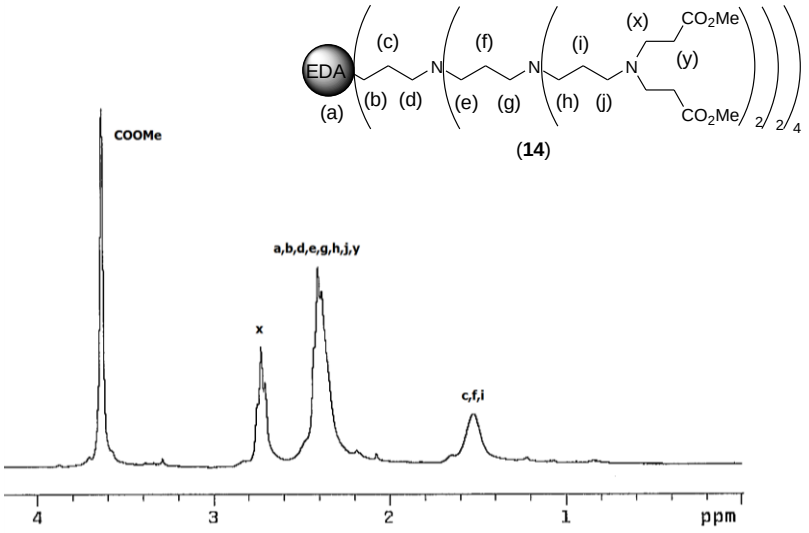

Figure S29. ^{1}H NMR spectrum of EDA-*dendr*-$(CO_2Me)_{32}$ (**14**) in $CDCl_3$.

I) EDA-*dendr*-$(CO_2Na)_{32}$ (15)

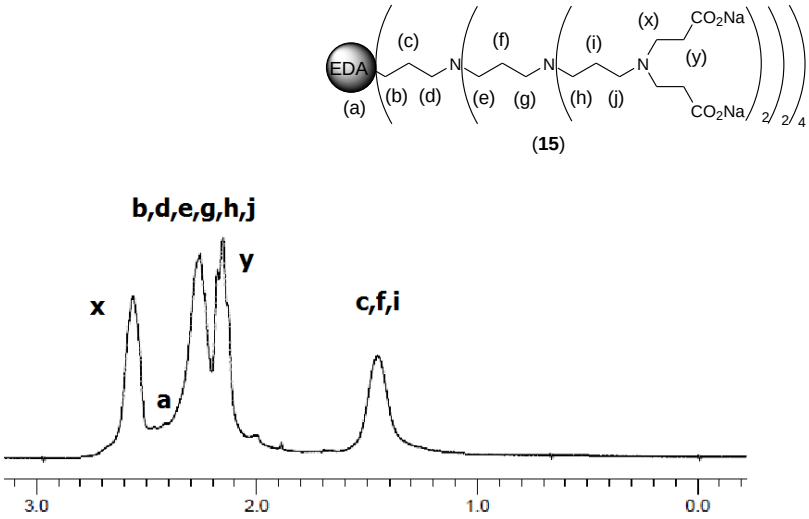

Figure S30. ^{1}H NMR spectrum of EDA-*dendr*-$(CO_2Na)_{32}$ (**15**) in D_2O.

- **UV-Vis spectra**

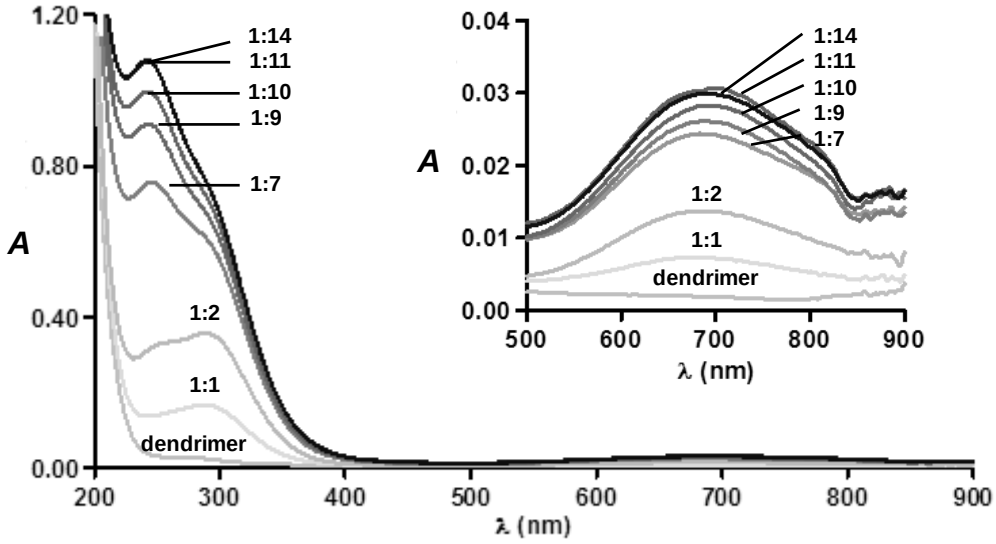

Figure S31. UV-Vis spectrum of copper titration of dendrimer EDA-*dendr*-$(CO_2Na)_{16}$ (**13**).

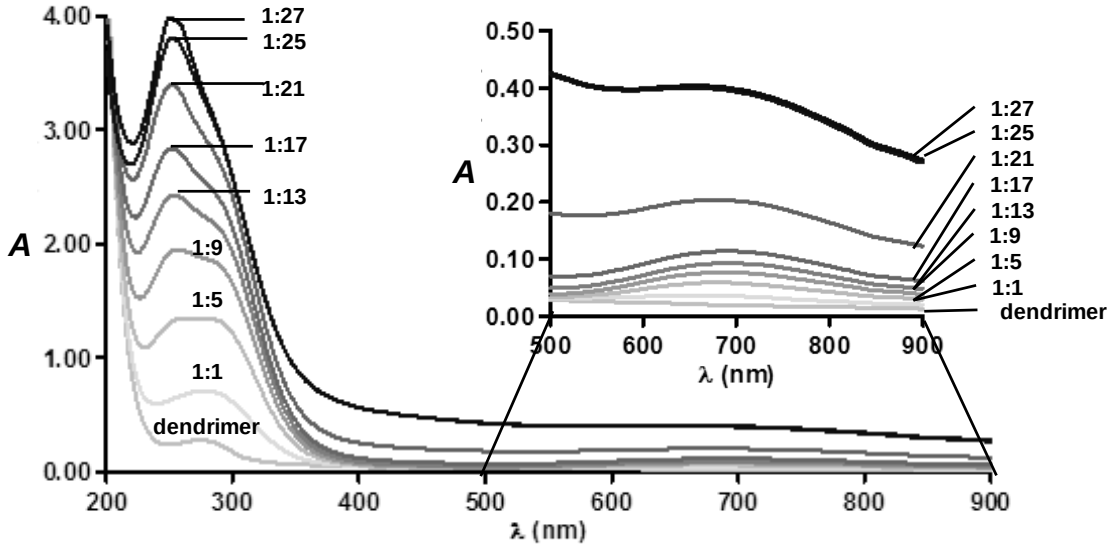

Figure S32. UV-Vis spectrum of copper titration of dendrimer EDA-*dendr*-$(CO_2Na)_{32}$ (**15**).

- **Potentiometric titration study**

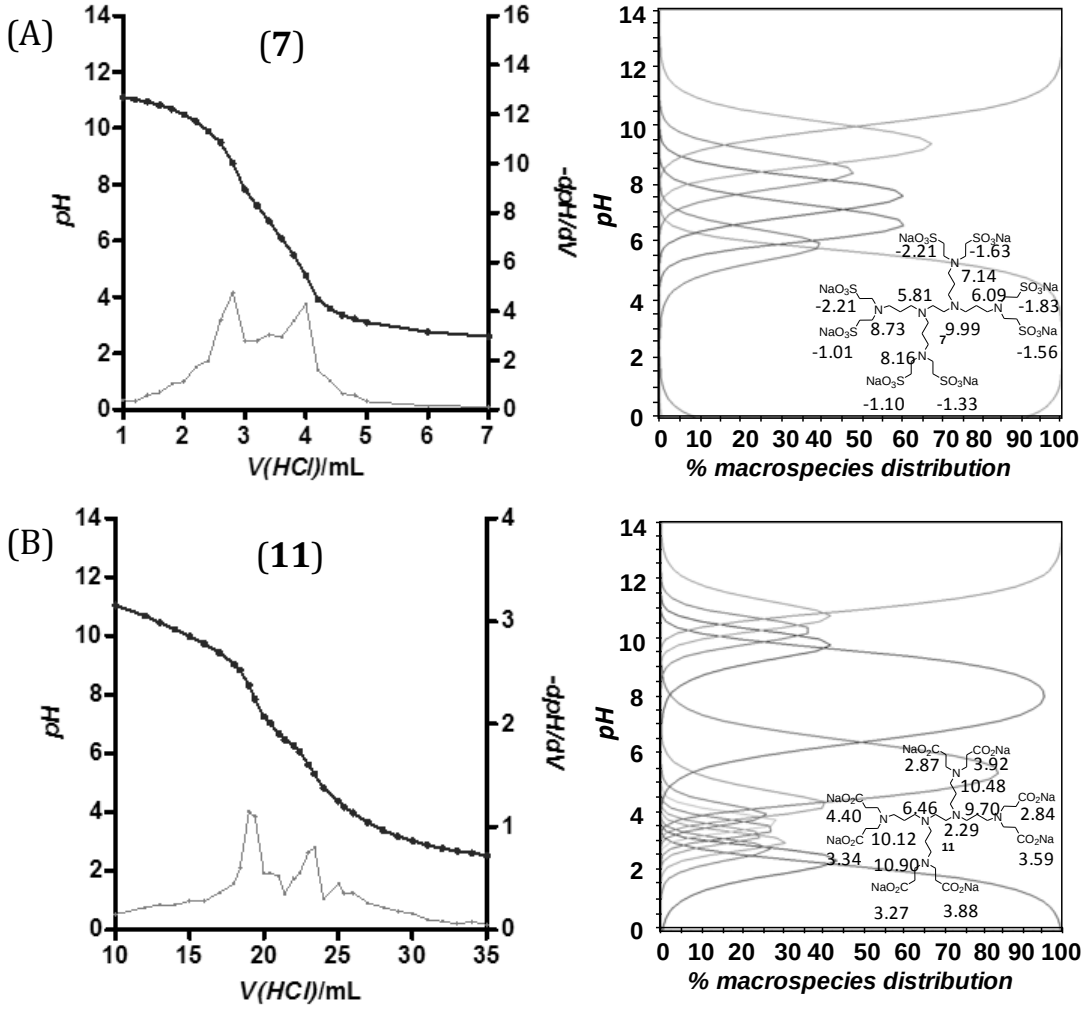

Figure S33. Experimental titration curves (left) and theoretical macrospecies distribution and pK_a calculation of each chemical group (right) of first generation dendrimers. A) EDA-*dendr*-$(SO_3Na)_8$ (**7**). B) EDA-*dendr*-$(CO_2Na)_8$ (**11**).